MISALIGNMENT EFFECT FUNCTION MEASUREMENT FOR OBLIQUE ROTATION AXES: COUNTERINTUITIVE PREDICTIONS AND THEORETICAL EXTENSIONS

Stephen R. Ellis*, Bernard D. Adelstein*, Kiwon Yeom**
*NASA, **San Jose State University Foundation
NASA Ames Research Center, Moffett Field CA 94035

The Misalignment Effect Function (MEF) describes the decrement in manual performance associated with a rotation between operators' visual display frame of reference and that of their manual control. It now has been empirically determined for rotation axes oblique to canonical body axes and is compared with the MEF previously measured for rotations about canonical axes. A targeting rule, called the *Secant Rule*, based on these earlier measurements is derived from a hypothetical process and shown to describe some of the data from three previous experiments. It explains the motion trajectories determined for rotations less than 65° in purely kinematic terms without the need to appeal to a mental rotation process. Further analysis of this rule in three dimensions applied to oblique rotation axes leads to a somewhat surprising expectation that the difficulty posed by rotational misalignment should get harder as the required movement is shorter. This prediction is confirmed. Geometry underlying this rule also suggests analytic extensions for predicting more generally the difficulty of making movements in arbitrary directions subject to arbitrary misalignments.

INTRODUCTION

Though instrumentation, training or procedures can be used to manage the control difficulties posed by awkwardly oriented teleoperation cameras, users of remote systems need to be able to operate through rotated views of the worksites to monitor automation. They also need to be prepared to take over in the event of failures. Indeed, in many cases the required instrumentation, sensors, and communication may simply not be present to enable the partial automation needed to provide users with intuitive geometric relations between their control inputs and movement of the end effector they control[1]. Consequently, there is a need to understand the scientific basis of the control difficulties encountered when telerobot users are faced with a rotation between the control frame of their input devices and their remote view of the worksite. This rotation constitutes a misalignment of two three-dimensional frames of reference. We call the function relating the amount of misalignment to the decrease in user performance the Misalignment Effect Function (MEF)[2].

We define the MEF as the relative decrement in the efficiency of user interaction with objects under user spatial control due to a rotation between their viewing or display coordinates and their input control co-ordinates. This decrement can be measured in a number of ways, but we have chosen to use normalized Path Length (nPL) for theoretical reasons apparent below. Normalized Path Length is defined for any movement from a starting point to a target as the path length actually moved divided by the minimum (straight-line) distance from the start point to the target (Ellis, Yeom, & Adelstein, 2012). Because nPL can be objectively related to optimal performance for purely translational movements, this definition also provides a means for extension to other aspects of movement since for these extensions all that is needed is an alternative optimality criterion. The movement in question then may simply be expressed as a proportion of the corresponding optimal movement.

In work reported last year (Ellis et al., 2012)) we have used nPL to measure the empirical MEF for pure pitch, roll or yaw rotations in an aeronautical coordinate system where yaw carries, pitch, carries roll with $+x$ forward away from the upright user's body. We demonstrated that pure roll rotations about the x-axis showed a distinctly more difficult pattern than pure pitch or yaw rotations about y and z respectively when results were integrated across all possible movement directions into the eight surrounding octants as described below. We argued that this difference may be due to the unique steering roles of pitch and yaw rotations versus roll for the lateral and vertical direction. Roll disturbs control in both the lateral and vertical directions while pitch or yaw only affect one of the two. This different performance under roll rotation awaits confirmation.

We were also able to show that the MEF's first ~1/3 of the MEF revealed a gradual loss of efficiency so that ultimately nPL approximately doubles as rotations approach ~65. We proposed a purely geometric argument that can explain this part of the MEF.

In the present paper we first review our previous results and derive our targeting rule in more detail. We then extend our measurement of the MEF in the experiment described below to rotations more representative of those actually encountered in the field in that they are not about canonical axes. In fact, the rotations that we have selected for the present experiment may seem more complicated than rotations about canonical axes because their descriptions in terms of Euler angles are not easily verbalized. We finally argue that such descriptive approaches focusing solely on the rotations themselves may need to be extended to include the user's specific control rule to fully understand their control difficulty.

Fig. 1 illustrates the basic movement task that we used. Participants were placed in a simple virtual environment. They were instructed to move their hand to a central starting point within a large wire-frame sphere. Next, following the participant's button press, a target would randomly appear some distance from the

[1] See Macedo, Kaber, Endsley, Powanusorn and Myung (1998) or design descriptions of the Intuitive Surgical *Da Vinci* telerobot for example of such partial automation.

[2] Formerly called the Misalignment Disturbance Function (MDF).

starting point. They were thereafter to manually move a cursor using their spatially-tracked right hand so as to make it touch the target, causing it to vanish. Participants would then return their hand to the starting point to prepare for the next target.

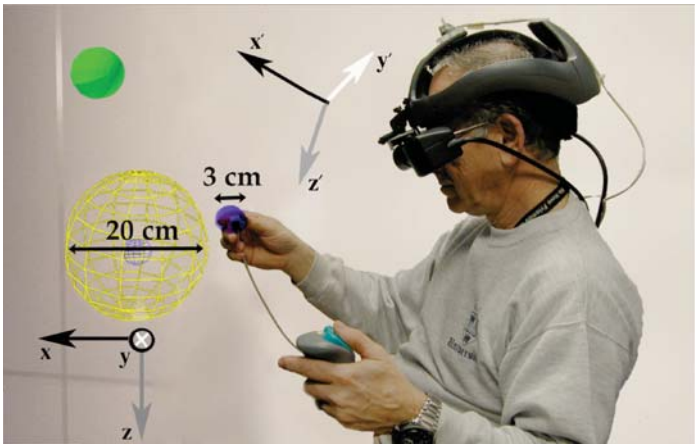

Figure 1. This composited exocentric view shows a participant in our immersing virtual environment moving a computer-generated blue cursor ball to touch the larger, flat-shaded green, spherical target at the upper left. Participants used a physical hand-held control to initiate trajectory recording and advancement to the next target (See Ellis *et al*, 2012 for details). The yellow wire-frame sphere encircling the start point, shown for scale, disappeared on trial start. The two coordinate frames, not visible during testing, show a multi-axis rotational misalignment between the display axes (lower left) and the control axes (upper left-center).

As in our previous work, our focus is on users' ability to overcome disturbances due to the unusual visual motion of their manually controlled cursor caused by experimentally imposed rotational misalignment. We believe the underlying control difficulty caused by control frame misalignment stems from the disturbed visual feedback that would otherwise help steer the user's motion. Consequently, to exclude rotational cueing information from visually or kinesthetically sensed structures in our experimental studies, we restrict ourselves to spherical display elements. Ultimately, we seek to develop a general theory that will enable us to predict the underlying control difficulty for user movement toward an arbitrary target location subject to an arbitrary rotational misalignment.

A Partial Theory of the MEF

Fig. 2 summarizes some results from last year's HFES Proceedings report in which the MEF was determined by pooling rotations about the canonical pitch, yaw and roll axes. The resulting function is usefully discussed in terms of the following three parts: the first slowly increasing part up to about $\psi = 65°$ of rotation, the second more rapidly increasing part leading to a peak somewhat greater than $\psi = 120°$, and a third with a distinctive decrease coming down to a level at $\psi = 180°$ that is well above that for 0° rotation. A complete theory of the MEF must explain all of these features—features that can also be seen in other earlier work. (Fig.2). We will focus only on the first part, below $\psi = 65°$, but will also comment in the Discussion section on rotations at and above $\psi = 90°$.

It is tempting to explain the MEF in terms of user internal information processing that might involve mental rotation. Such processing may well be involved, especially in the presence of larger rotations. However, since the disturbance of user performance is inherently geometrical, it is informative to first look towards geometrical explanations that may involve simple targeting rules.

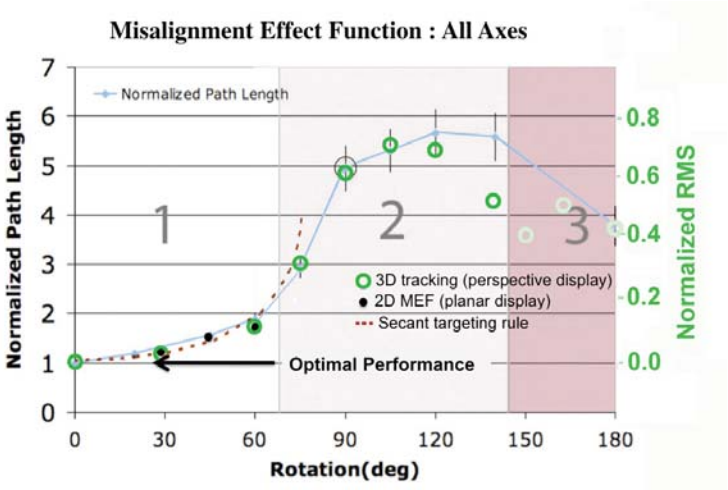

Figure 2. The MEF resulting from pooling results from Ellis, Yeom, & Adelstein (2012) for rotations about pitch, roll, and yaw for a task like that in this paper. For comparison, previously published results (Ellis & Adelstein, 2009) from a related 2D placement task are overlaid. Also overlaid are results from a 3D tracking task done with a perspective display that subject to display-control coordinate misalignments (Ellis, Tyler, Kim & Stark, 1992). The three data sets show similar MEFs.

In particular, we have examined a targeting rule that essentially is a definition of visual-motor coordination. It assumes human movements are made of submovements as posited by classic sample-data control movement models (Stark, Iida & Willis, 1961). The rule is as follows: First, set the current kinesthetic direction for each submovement, $\mathbf{x}_i$, equal to visual direction at each submove¬ment start, $\mathbf{d}_i$. Second, iterate across all submovements, making the kinesthetic direction equal to the estimated visual direction at each submovement until target contact (Fig.3). Implicit in this rule is that completed movement paths consist of a sequence of progressively refined submovements arising from the sample-data control at the heart of vertebrate kinesiology (e.g., Stark et al, 1961; Crossman & Goodeve, 1983).

As shown for the planar case depicted in Fig. 3, integration across all of a movement's constituent submovements yields a simple expression for the expected nPL. Since $1/\cos(\psi) = \sec(\psi)$, we call this expression the *Secant Rule* for coordinated hand movement. In fact, this targeting defines an equivalence class across velocity since a wide variety of velocity profiles will give rise to the same general trajectory form, though the piece-wise approximation to the equiangular spiral will vary. This equivalence class over a variety of velocity profiles is directly analogous to the equivalence class over ratios of movement distances to target widths defined by Fitts's Law[3]. One can see in Fig. 2 that the targeting process provides a fairly good fit to the empirical MEF for rota-

[3] Deeper connections to Fitts's Law exist showing that target width plays the role of a normalizing factor but they are out of this paper's scope.

tions less than ~65°, and does so without free parameters! Clearly, this simple targeting must break down at some point since sec(ψ) → ∞ as ψ → 90° where the targeting rule results in an orbit around the target. Therefore, the underlying targeting process must change beginning at or near this rotation angle.

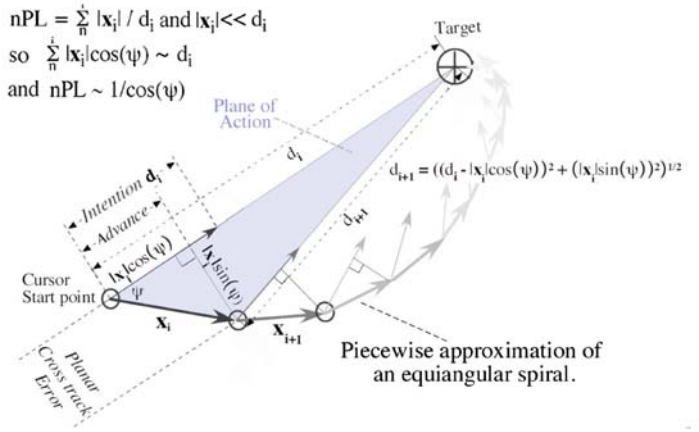

Figure 3. Iterative targeting geometry for the *Secant Rule* is sketched where $intention_i = \mathbf{x}_i$. Shaded (blue) indicates the *plane of action*.

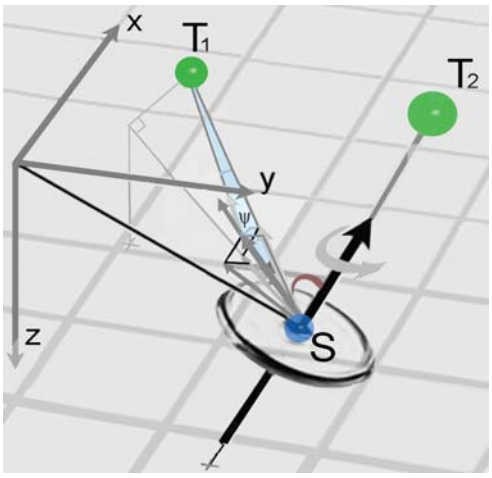

Figure 4. The targeting rule is visualized more generally in 3D space showing the instantaneous *plane of action* (light blue shaded triangle) determined by the intended direction of movement (light vectors) and the achieved direction of movement (darker vectors).

The range of conditions over which of the proposed targeting rule applies is probably determined by an optimization process analogous to that suggested for raptors that move, i.e., fly, along equiangular spirals when they dive onto their prey. They do so because from their normal surveillance height they must target their prey using the higher-resolution of their two foveas, which is rotated laterally ~45° with respect to their body axis (Tucker, 2000). It appears the birds fly time-optimally by trading off the longer flight path needed to maintain use of this fovea against the added speed they can achieve by avoiding head turning that would slow them due to drag. Human telerobot operators may similarly trade off the time to move along an equiangular spiral against the added time and effort needed to determine a compensatory path. This tradeoff may be reasonably expected since arm control models are frequently time optimal. The operative ratio that may influence the human user's tradeoff is the *advance / intention* ratio as indicated in Figs. 3 and 5. This ratio is, in fact given by cos(ψ), where ψ is the rotation angle. Data analyses suggest the critical value for this ratio to successfully predict performance is around 0.56, which corresponds to cos(65°). Thus, 65° is approximately the largest rotation for which the *Secant Rule* applies. The critical value could be interpreted as the minimum acceptable efficiency factor with which the *advance* brings the operator's controlled element towards their targets (Fig. 3, 4 and 5). Interestingly, this factor is reminiscent of the constant, A, used by Crossman and Goodeve (1983) in their derivation of Fitts's Law, where A represents the proportion of the remaining distance moved to the target during each submovement. This parallel suggests the development of a Fitts's Law equivalent for off-axis movement.

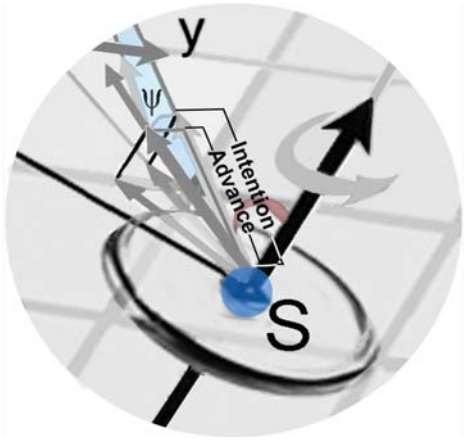

Figure 5. Enlargement of targeting rule visualization in 3-D space. The rotation, Ψ, of the intended movement vector (lightest arrow) to the achieved movement vector (dark arrow) defines the blue *plane of action.*

Curiosity regarding generalization of the MEF to rotations about noncanonical axes naturally arises and we have begun to investigate more generalized conditions in the following experiment. In order to think about the possible effects of such rotations on the MEF we have extended the geometry of Fig. 3 to three dimensions in Fig. 4. This figure represents an arbitrary rotation associated with an arbitrary motion from start point S to target T_1. The rotation axis is represented by the thick dark black arrow passing through S. The arc around the axis (ψshows the amount of rotation. The plane of rotation is represented by a disk centered at S. Any possible rotation may be represented as done in Fig. 4.

For rotations that we previously used about the canonical axes, all planes of rotation were *ipso facto* parallel to the canonical surfaces orthogonal to the rotation, e.g., roll rotation about the x-axis has a plane of rotation parallel to the *y-z* plane. These rotation conditions are relatively easily described and understood by participants. But they are very special cases. A full theory of the MEF must extend beyond them to the situation shown in Fig. 4.

Consideration of Fig. 4 as representing an arbitrary rotation leads to some qualitative conclusions from the geometry that we investigate in the experiment below, deferring a more quantitative analysis for future reports. For example, one can immediately see that the specific position of the target with respect to the rotation axis has a major influence on the effect of the rotation: Targets located exactly on the axis, e.g., T_2, are unaffected by the rotation. Those within plane of rotation it, are maximally affected, and

correspond to the analysis in Fig. 3. Another interesting inference, however, is that targeting using the rule from Fig. 3 will result in a three-dimensional spiral path. The simulations and closed form equations describing this path will be treated in future reports. Significantly, for those rotations for which the *Secant Rule* applies, the spirals are locally roughly planar. One may think of them as approximations of the planar spirals within a *plane of action* in that their length is closely predicted by the planar analysis used in Fig. 3.

It is interesting to note that there is a great advantage for participants who can stay in an initial *plane of action* shown in Figs. 4 and 5. Staying in this plane turns their targeting task into a simpler one-de¬gree-of-freedom (dof) problem instead of a two-dof problem if they leave the plane. Accordingly, because displacement noise that takes the cursor out the *plane of action* has a much greater effect on the directional corrections needed to return to the plane as the cursor approaches the target, one might expect targeting to become more difficult for nearer targets than for farther ones. This effect is enhanced by the slowing of cursor motion as one gets closer to the target, which, in turn, makes visual discrimination of the error more difficult. We investigate this possible effect of distance in the following experiment.

METHODS

Subjects: Ten unpaid volunteers (eight men, two women) aged 24-65 participated. Subjects were screened for stereo vision, compatibility with the head-mounted display and provided IRB required consent for human experimentation.

Head mounted display: A modified Rockwell-Collins SR80 binocular head mounted displays was used. Descriptive details may be found in our previous paper (Ellis et al., 2012) and manufacturer specifications

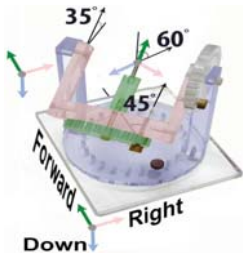

Figure 6. Fick gimbal illustrating a yaw-pitch-roll Euler sequence for one of the rotations used in the experiment.

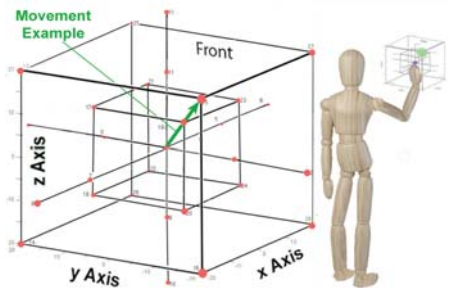

Figure 7. Approximate positions of the 28 targets used for the two target distances shown by spherical red markers. Movements were from the center outward. Separate randomized sequences of targets with a fixed rotation were used for blocks of targets for each participant.

Computer hardware and software: The experiment was run in a custom virtual environment (VE) authored by Richard H. Jacoby, using lower-level tracking sensor interface software by AuSim, Inc. under Windows XP (SP2), rendering at 60 fps, with a measured full system latency of ~30 ms. See (Ellis, et al., 2012).

Experimental virtual environment: The VE created for the study was a simple room with dimensions roughly matching the physical room (4.0 x 4.5 x 2.9 m) in which the experiment was conducted. Diffuse lighting coming from virtual room sources mimicked the lighting in the real room. Texture maps that corresponded approximately to the room's actual ceiling and floor provided some additional realism.

Experimental design: A more detailed description of our general experimental procedure may be found in our previous paper (Ellis, Yeom, & Adelstein, 2012). It is important to reiterate here that the participants were told that when their task got harder, the goal of their movement was to try to move as they did when the task was easy during initial familiarization. We put no specific premium on quick motion onset, speed, or accuracy.

Independent variables. 1) Target distances from the origin centered in front of the participant at two levels were 11 cm or 22 cm. Target locations are shown in Fig. 7. 2) Control-to-display coordinate rotations in terms of yaw, pitch, and roll angle were, respectively, (±45°, 35°, 0°), (±45°, 35°, ±30°), (±45°, 35°, ±60°), and (±45°, 35°, ±90°). (See Fig. 6 for sample pose). Note that the signs for yaw and roll angles were matched for each Euler triple, yielding eight rotation levels. This sign matching resulted in symmetrical poses of the final Euler rotation axis[4], e.g., (+45°, 35°, +30°) is symmetric with the triple (−45°, +35°, −30°). Ultimately, we collapsed rotation across signs, as we found no reliable asymmetries in the performance data.

Dependent variables: Normalized Path length (nPL) was used as our principal dependent measure. It is a kind of efficiency measure, essentially a percent calculation that we infer also reflects task difficulty on the presumption that participants are consistently striving for the same efficiency when they "try to move as they did when the task was easy."

RESULTS

Fig. 8 plots the two significant main effects confirming the somewhat counterintuitive prediction that, at least in terms of nPL, movement towards the near targets is relatively longer and less efficient. There was no statistical interaction as is evident from the parallel traces of the two presented distance conditions. Note that the final 90° rotation in the Euler sequence (i.e., roll) has a much smaller impact on performance than a single 90° about a canonical axis shown in Fig. 2.

DISCUSSION

Because the present somewhat counterintuitive results are based on presumptive constant noise or jitter present in human motion, they emphasize that any full theory of the control difficulty introduced by a display-to-control rotation needs not only to predict the biases in errors but also the variances that are introduced. In this context we have observed in our data that variances in normalized Path Length for the first part of the MEF are a linear function of the introduced rotation. We plan to include this aspect of our data in future more complete targeting models as we lack adequate space in the present report

[4]We refer to symmetry of the Euler axes.

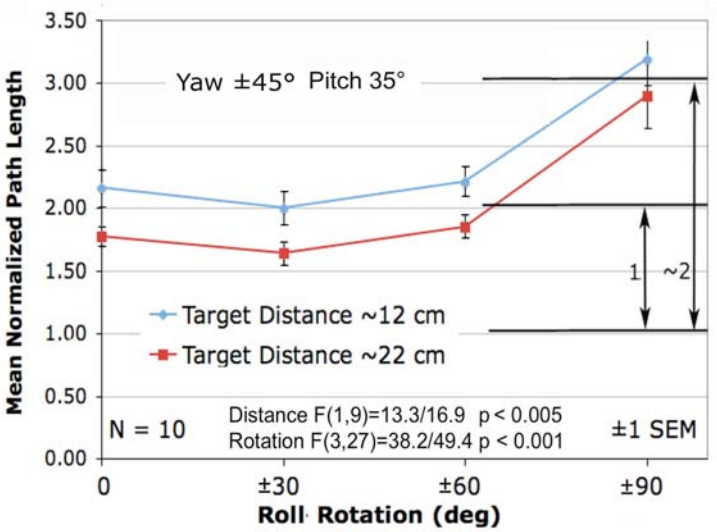

Figure 8. Results for ANOVA F's for skew-corrected log transformed data shown respectively. Performance ranged over about a factor of two with respect to optimal performance where nPL = 1.

A second observation that we can make is based on a comparison of performance under pure pitch, yaw, or roll rotations of 60° and 90° from our prior study (Ellis et al., 2012) versus performance in the present experiment where roll (the third component of our Euler rotation sequence) of the same magnitude is instead applied on top of underlying yaw and pitch rotations. Despite the fact that the resulting poses in the present experiment are much more difficult to describe, our participants' behavior was much less affected by these compound Euler rotation sequences than pure pitch, yaw, or roll.

Our analysis of this surprising result is not complete. The principal difference we have identified so far is that though the amount of twist about the rotation axis, (90.4°) is very close to that used for the canonical axes rotations of the previous experiment, the axis of this rotation has an azimuth of 140° and elevation of 5°. This direction places it far away from alignment with any canonical axis and it may be a privileged direction with respect to the participants' body. In future work we plan to examine explicitly the orientation of the rotation axes with respect to the participant's body to evaluate this factor systematically.

A final comment regarding our *Secant Rule* is noteworthy in that it provides an explanation for a phenomenon reported by Abeele and Bock (2001). When testing transfer of sensorimotor adaptation to rotational misalignments, they noticed that participants who adapted to fixed rotations less than 90°, showed transfer to other rotations less then 90° but not to rotations greater than 90°. Conversely, those adapting to rotations greater than 90°, only showed transfer to other larger rotations. Our rule implies this pattern. Transfer from small to large rotations does not occur because no amount of training will make the *Secant Rule* work for large rotations. Clearly, a different rule must be used for large and small rotations.

In the end it may be necessary to appeal to "mental rotation" as an explanation for some aspects of the MEF, but we hope, those who take this approach, ourselves included, realize the violation of Occam's Razor that such a tack involves. Appealing to a concept itself not well understood hardly promises an explanation that could have the ring of truth. In any case there are specific difficulties in any appeal to mental rotation. Careful measurement of the MEF generally shows that as the rotation angle increases past 120° towards 180° there is a clear decrease in the function, which indicates that the task gets easier. This drop seems to be associated with motor performance (Chintamani et al, 2010). Classic mental rotation functions, in contrast associated with perception or discrimination, continue to increase consistent with the idea that a more or less constant rate of mental rotation produces a continuous increase in the participants' response times (Shepard & Metzler, 1971, but see Collishaw & Hole, 2002).

It must be noted, however, that the decrease of the MEF for larger rotation angles may not be seen in studies without sufficient statistical power or appropriate experimental design to reduce the significant noise associated with function measurements of large rotations. Indeed, any explanation of this later (i.e., >120°) part of the function also needs to explain this increased noise. Our expectation in this respect is that the noise arises from ambiguities and uncertainties as to the orientation of the error vector when submovement targeting errors are noticed. These ambiguities, which may amount to errors in understanding the local reference orientation of the *plane of action*, could result in large incorrect "corrective" movements out of the initial *plane of action* and could, by an argument similar to the one we've made about the target approach, also explain the rise in trajectory variability for the large rotations.

Acknowledgment: This work was funded by the NASA Human Research Program's Space Human Factors Engineering Project.

REFERENCES

Abeele, S. & Bock, O. (2001) Sensorimotor adaptation to rotated visual input: different mechanisms for small vs large rotations. *Exp. Brain Res., 140*, 407-410.

Chintamani, K. K., Cao, A. Ellis, R.D. & Pandya, A.K. (2010) Improved telemanipulator navigation during display-control misalignment using augmented reality cues. *IEEE Trans. Sys. Man & Cyber. Sys. & Humans, 40(A)*, 1, 29-39

Collishaw, S.M. & Hole, G. J.(2002) Is there a linear or nonlinear relationship between rotation and configural processing. *Perception, 31,* 287-296.

Crossman, E.R.F.W. & Goodeve, P. J. (1983) Feedback control of hand-movemen and Fitts' law. *Quarterly J. Exp. Psych., 35A*, 251-278.

Ellis, S. R., Tyler, M., Kim, W. S., & Stark, L. (1992) Three-dimensional tracking with misalignment between display and control axes. *SAE Transactions: J. Aerospace, 100-1,* 985-989.

Ellis, S.R. & Adelstein, B.D. (2009) Kinesthetic compensation for sensorimotor rearrangements. *J. of Motor Behav., 41,* 6, 501– 518.

Ellis, S.R., Yeom, K. & Adelstein, B.D. (2012) Human control in rotated frames: anisotropies in the misalignment disturbance function of pitch, roll, and yaw. Proc. HFES, October, pp. 1336-1341.

Macedo, J.A., Kaber, D.B., Endsley, M.R., Powanusorn, P., & Myung, S. (1988) The effect of automated compensation for incongruent axes on teleoperator performance. *Human Factors, 40*, 4, 541-553.

Stark, L, Iida, M. & Willis, P.A. (1961) Dynamic characteristics of the motor coordination systems in man. *Biophysical Journal, 1*, 279-300.

Shepard, R & Metzler. J. (1971) Mental rotation of three dimensional objects. *Science, 171,* 972, 701-3.

Tucker, Vance A. (2000) The deep fovea, sideways vision, and spiral flight paths in raptors. *J. Exp. Biology, 203*, 3745-3754.

Yeom, K. Adelstein, B.D., & Ellis, S.R. (2012) Determining the discontinuities for three-dimensional trajectory data in teleoperation. *Proc HFES*, October 2012. pp. 2537-2541.